Journal of Physics:
Conference Series

PAPER • **OPEN ACCESS**

Mechanical design of a quartz oxy-combustion chamber: chemical-physical analysis of the combustion phenomenon

To cite this article: Raho Brenda *et al* 2024 *J. Phys.: Conf. Ser.* **2893** 012111

Journal of Physics: Conference Series **2893** (2024) 012111 doi:10.1088/1742-6596/2893/1/012111

Mechanical design of a quartz oxy-combustion chamber: chemical-physical analysis of the combustion phenomenon

Raho Brenda[1], Milanese Marco[1*], de Risi Arturo[1] and Colangelo Gianpiero[1]

[1] Department of Engineering, Institution, City, Country

[*]E-mail: marco.milanese@unisalento.it

Abstract. Climate change and environmental degradation are huge threats to Europe and to the world. To overcome these problems, there are a series of government proposals with the aim of achieving carbon neutrality, or, at least, reducing net greenhouse gas emissions up to 55% by 2030. The greenhouse effect is caused by a high concentration of harmful emissions, especially CO_2, in the atmosphere; hence, it is imperative to minimize their amount. Because of this, there is a strong effort to research suitable operational methods and secure useful technological advancements. A valid solution to actively contribute to the global objectives for achieving carbon neutrality is the oxy-combustion process, i.e., combustion in an oxygen atmosphere. This process can be considered as "clean" combustion because it does not produce pollutants such as NO_x and SO_x but only CO_2 and steam. In addition, the production of essentially pure CO_2 makes possible subsequent operations of carbon sequestration. The proposed paper describes the mechanical design and construction of a lab-scale oxy-fuel chamber, entirely made of quartz. The chosen material makes it possible to visualize, analyze and study the combustion process inside the chamber through imaging techniques by investigating its chemical and physical characteristics.

1. Introduction

Fossil fuels were responsible for the first half of the 20th century's emissions for a large portion of the world's energy. Particularly coal has been considered the most cheap and plentiful resource, when measured against all other fossil fuels, including natural gas and oil [1],[2]. As the most plentiful, readily available, and reasonably priced fuel, coal is also the most dependable and easily accessible energy source. It plays a critical role in global energy security and is a key component of the economic and social advancement of highly populated countries like China and India [3],[4].

Although renewable energy sources are being researched, around 81% of energy consumption still comes from fossil fuels. This has caused problems with atmospheric CO_2 emissions on a global scale because of the following combustion reaction:

$$C_nH_m + (n + m)O_2 -> nCO_2 + \frac{m}{2}H_2O \quad (1)$$

As it is well known, CO_2 is then released into the environment in a volume equal to the amount of carbon involved in the reaction. Nevertheless, this does not align with the 2030 emissions

reduction target set by the European Union and the 2050 goal of becoming the first continent to achieve carbon neutrality [5],[6].

These factors need a rapid advancement toward nearly zero-emission technologies such as renewable energy or the use of Carbon Capture Sequestration (CCS) techniques [7], which can be based on:

- Pre-combustion processes, in which fuel and comburent are treated before the combustion reaction to avoid the production of pollutants.
- Post-combustion processes, whereby only the combustion products are treated to avoid the emission of pollutants into the environment.
- Oxy-combustion processes, i.e., combustion reactions in a pure oxygen environment.

The oxy-combustion is a very effective technology that attempts to decrease emissions of environmental contaminants while enhancing combustion reaction performance [8],[9]. Although there are not any industrial plants with oxyfuel technology, the process has been the subject of numerous investigations, including some experiments that shed light on design parameters and operating issues.

Compared to conventional combustion reactions, the oxygen-combustion reaction is more efficient: higher temperatures, increased CO_2 concentrations downstream, and reduced fuel consumption are all possible. The oxyfuel process has special characteristics that have positive effects on the efficiency of the reaction [10]:

- the high-pressure operation causes the temperature condensation of water steam in the exhaust gas to be higher, resulting in more efficient latent heat recovery [11];
- the energy required for CCS is reduced because CO_2 is delivered at high pressure [12];
- it is possible to decrease the size of the heat exchanger because the exhaust gases have a higher convective heat transfer coefficient [4].

Furthermore, oxy-combustion produces fewer pollutants due to controlled combustion between fuel and pure oxygen. Specifically, there will be a notable drop in NO_x at the exhaust, due to the absence of Nitrogen, which is mostly found, instead, in the atmospheric air.

Replacing air with pure oxygen results in different temperature and heat flux distributions during the combustion reaction because the Nitrogen (in the air) has a different thermo-chemical behavior than Oxygen. Besides, the triatomic molecule CO_2 (this gas enters the combustion chamber as recirculation gas) differs from nitrogen in several significant physical and chemical ways, there are changes in thermodynamic parameters that account for the variances in flame morphologies between air-fired and oxyfuel-fired flames.

By using numerical analysis, Choi [13] and Yin [14] examined the structure of a CH_4-O_2 edge flame and contrasted it with the CH_4-air edge, observing a noticeable difference between them.

Due to the different chemical composition of exhaust gases, the oxyfuel process's heat transmission differs from that of traditional combustion. Triatomic gases (CO_2 and H_2O) are the byproducts of burning oxyfuel, and unlike diatomic gases (N_2), they are less transparent to radiation. Furthermore, their partial pressure is extremely high, which raises the exhaust gases' emissivity and absorption.

In their investigation on laminar flame, Chen *et al*. [15] found that the adiabatic flame temperature and propagation speed in an O_2/CO_2 environment are lower than those found in an air atmosphere. Moreover, they observed that these values rise as CO_2 levels rise; specifically, the latter's temperature peak drops by roughly 200 K [16].

There are other parameters that could influence the physics of the reaction such as the concentration of oxygen used in combustion or the percentage of recirculation gas.

Bejarano [17] and Levendis [18] investigated how burnout times were affected by oxygen concentration. In general, the temperature of the flame affects the duration of combustion for concentrations higher than 21%. Burnout times decrease when the temperature of combustion and the concentration of oxygen both rise simultaneously. The combustion time progressively reduces to 8–17 ms at 2100–2300 K with 50% of O_2 and to 6–13 ms at 2300–2400 K with 100% of O_2.

The percentage of recirculation gas is the most crucial parameter in the oxyfuel process. Because it is used to dilute the combustion agent, changing the heat transfer characteristics, the response time, and altering combustion efficiency, it is regarded as a vital instrument for controlling combustion.

The impacts of the recycling ratio on several metrics, including the convective heat transfer coefficient, radiative heat flux, and adiabatic flame temperature, were investigated in 2010 by Smart *et al*. [19]. Their research displayed the peak normalized radiative heat flux and the normalized computed flame temperature as a function of the effective recycled ratio during an oxyfuel process. Specifically, the convective heat flux rose as the recycled ratio grew, but the radiative heat flux maxima showed an inverse relationship with the recycled ratio.

Through their research in a combustion reactor, Molina *et al*. [20] proposed in 2005 that CO_2 delays the igniting of coal and char and affects the length of devolatilization. The rise in oxygen concentration is what causes this impact since it speeds up particle ignition in the atmospheres of N_2 and CO_2. Additionally, they looked at the effects of increasing oxygen concentrations at various temperatures and found that, the 1650 K process follows the same pattern as the 1200 K process, but with a minor flame instability and a flame igniting delay.

Considering the numerous studies, it was decided to build a laboratory setup of a small 6kW oxy-fuel system in order to investigate what happens during an oxy-fuel reaction from a chemical and physical point of view, how the distribution of the flame varies inside the oxy-combustion chamber and at what temperature it develops. This was possible through imaging techniques and the analysis of the emission spectrum of the flame detected with a monochromator.

2. Spectroscopy analysis

Molecular spectroscopy is a theoretically very complex discipline, characterized by a high variability caused by the intrinsic mutability of the state of the molecules and the changeability of the external conditions of the system. The chemical and physical properties of molecules depend, in fact, on numerous factors, such as the type of atoms that constitute them, the type of bond, the type and level of involved excitation. Through the analysis of the spectra of substances, it is, therefore, possible to reconstruct the structure of a molecule, i.e. to trace its chemical-physical characteristics.

Analysing of spectral lines, molecular spectroscopy makes it possible to identify the chemical species present in a sample. These are produced as a result of electromagnetic waves interacting with materials; these interactions can result primarily in emission- or absorption-related phenomena.

In the present work, since emission phenomena of electromagnetic radiation from the flame are present, numerous analyses of the emission spectra of matter have been carried out. Particularly, through analysis of emission peaks, it was possible to identify the substances that develop in the combustion process, as there is a direct correspondence between the wavelengths of the emission peaks and the reaction compounds, as shown in the Table 1.

Table 1: Wavelengths of absorption/emission peaks for different molecules

Molecule	Wavelength
C_2	385.2 – 410.2 - 473.7 – 516.5 – 589.9
CH	431.4
C_2H_2	228
C_4H_2	506
C_6H_6	273-425 - 460
CHO	329 - 337 – 350-613
CHOOH	239
CH_2O	290-395 - 424
CH_3O	351 - 364
CO	240-280-451 – 483 – 519- 561 – 608-640 – 651.3 – 679.9
CO^+	229- 375- 395.3 – 425.2 – 427.4
CO_2	220-230-257-391 – 441 – 455 – 465 – 478 – 493 – 519 – 531
O_2	321 - 337 - 351.7 – 367.1 – 759.3
OH	306.6 - 308.9 – 775.5

3. Experimental setup

3.1 Combustion chamber geometry

For the design and sizing of the oxy-combustion chamber, the resistance to the high temperatures and pressures characteristic of the process was considered.

The oxyfuel chamber, reported in Figure 1, has a central cylindric core consisting of a quartz tube, type NHI 1100 by Helios Quarz Italy. The decision to make the combustion chamber entirely of quartz and not with a metal material is related to the possibility of optically studying the flame during the combustion reaction.

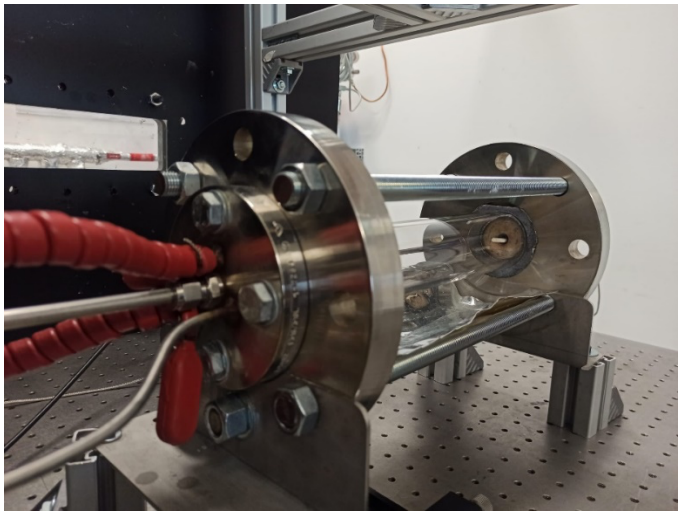

Figure 1: Design of the geometry of the combustion chamber

The chamber has an outer diameter of 60 mm and an inner diameter of 50 mm, 300 mm long and 5 mm thick.

The minimum tube thickness was determined according to the sizing standards for mechanical components. It was considered the fragile nature of the quartz, the high temperatures to which it is subjected (approximately 1200°C), and the operating pressure (5 bar).

Quartz has a low coefficient of thermal expansion, equal to $5.5*10^{-2}$ cm/cm °C, and has high thermal stability compared to traditional glasses. Besides, a particular characteristic of quartz is that it does not have a specific melting temperature, but softens at around 1630°C, behaving like a plastic material.

The cylindrical chamber is completed by two PN40-DN80 flanges in AISI 316 stainless steel. These flanges are held together by four M16 tie rods and tightened with M16 nuts. All components are in AISI 316 stainless steel.

The connection between the quartz tube and the stainless-steel flanges is made by compression and its tightness is guaranteed through the use of graphoil gaskets.

Inside of the inlet flange, there is a turbulator in AISI 316 of dimensions 50mm*24mm. The turbulator has the axial inlet of the methane in the center and a series of radial blades to generate the swirl motion of the incoming gases.

Gas inlet occurs through a flanged connection. As seen from Figure 2, the input flange has four inlets. The central duct is dedicated to methane. It has a stainless-steel nozzle having a 1 mm diameter orifice as its terminal.

Proceeding radially to the flange, there are the other three gas inlets, placed at 120° to each other for oxygen, carbon dioxide, and steam.

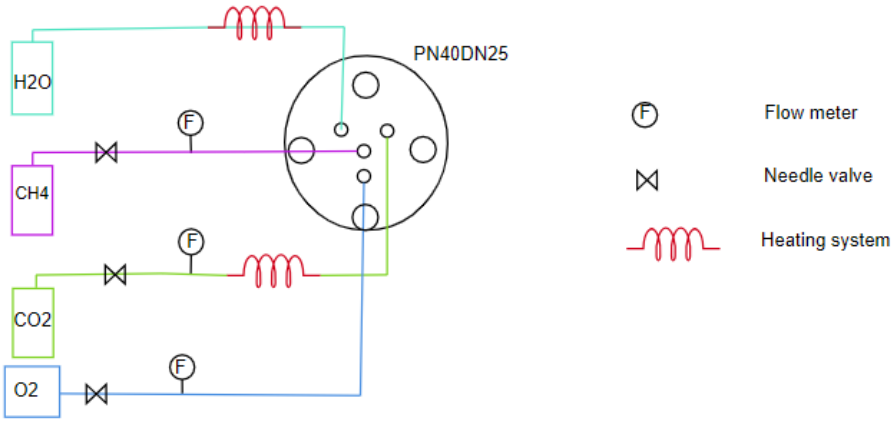

Figure 2: Gas inlet line

CO_2 and H_2O are introduced to simulate the recirculation of exhausted gases. For this reason, before being introduced into the combustion chamber, they undergo preheating with heating resistors in such a way as to introduce the gases at a temperature of 250°C. The heating of the aforementioned gases is regulated and controlled through an *ad hoc* developed Labview software.

Methane and oxygen on the other hand, do not undergo any treatment before entering the combustion chamber.

The three gases, oxygen, carbon dioxide and steam, at the end of their pipes, enter into a cylindrical mixing chamber placed in the central part of the flange: in this zone, the three gases mix.

After exiting this chamber, the gases pass through a finned turbulator capable of providing a swirl motion to the gas stream.

The exhaust gas outlet is unique (Figure 3) and is used to introduce a platinum/rhodium thermocouple to measure the temperature inside the combustion chamber.

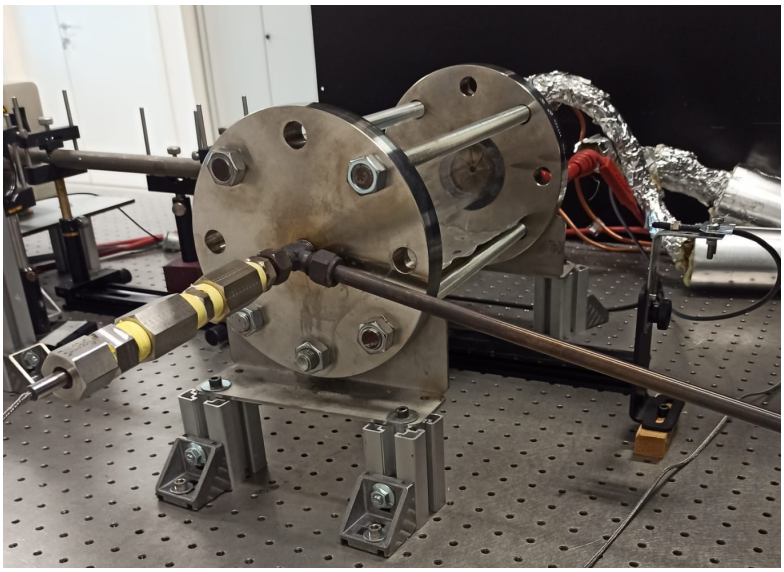

Figure 3: Gas outlet line

Downstream of the outlet, there is a gas cooling system, capable of condensing the vapor present in the gases. Therefore, the water is separated from the hot gas (mainly composed of carbon dioxide) and collected in a small tank.

3.2 Optical analysis setup

The analysis of a flame is based on the emission spectrum, identifying the species of molecules, and tracing their temperature and concentration.

Figure 4 shows the schematic of the experimental setup for spectroscopy analysis, where L represents the biconvex lens, F1 is an optical fiber that converges into the monochromator, CC is the CCD controller that drives the CCD head and download data coming from the same CCD to the computer, Andor is the intensified Andor camera coupled with 310 nm band pass filters, which allows acquiring images related to OH radicals inside the oxy-combustion chamber.

Combustion inside the chamber is ignited by a spark, generated by a high energy pulsed laser Nd: YAG with a pulse amplitude of 8 ns, a frequency of 10 Hz, and a length of the emitted photons of 1064 nm, near-infrared region. Particularly, the emitted laser beam is passed through a biconvex F100 lens with the aim of focusing it at a distance equal to 100 mm in the focus of the lens, generating a spark.

The light from the oxy-combustion chamber is collected by an optical fiber, reaching the monochromator and then subsequently the CCD which in turn supplies the signal to the computer. With the Spectra software it is possible to see the flame emission spectrum.

The monochromator is responsible for breaking down the polychromatic white light into a dispersion of monochromatic bands. This conversion is achieved by interacting the light with a diffraction grating which breaks it down into its components. This element, when illuminated by collimated non-monochromatic electromagnetic radiation, behaves like a multiple source thanks to its slits and created constructive interference. Th HR-460 monochromator was used in the analysis in which:

- Polychromatic light passes through the entrance slit.
- It subsequently affects the collimating mirror and produces a polychromatic parallel light;
- The polychromatic light reaches the grating that separates the spectrum into monochromatic bands equidistant from each other.
- The monochromatic parallel beam then impacts on a mirror which focuses and reflects the light towards the exit slits.

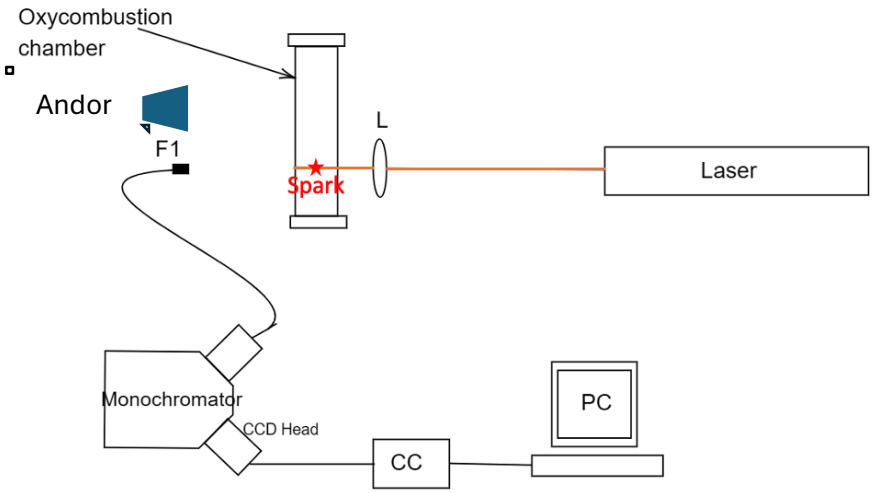

Figure 4: Schematic of the experimental setup for spectroscopy analysis. L are biconvex lenses, F1 is an optical fiber, CC is the CCD controller, Andor is the intensified Andor camera.

Each component with its own wavelength affects the output plane with an angle and the grating rotates automatically via software in such a way as to star scanning the wavelengths giving rise to a spectrum in a chosen range.

For each scan carried out, i.e. for each rotation of the grating, the monochromator generates a spectral dispersion equal to approximately 30nm with a resolution of less than 0.05nm at 546nm. The accuracy of the wavelength determination is very high ±0.15nm which introduces very low measurement errors. Subsequently, the monochromatic light coming out of the monochromator reaches the image intensifier of the ICCD 3000V which has the task of transforming a light signal into an electrical signal providing a measurement of the intensified photon flux.

As the CCD intensification factor increases, the background noise increases, and therefore this must be considered during the subsequent analysis of the experimental data. The intensification system activates and deactivates in the order of nanoseconds and its acquisition system has a very high quantum efficiency of approximately 20%. Quantum efficiency is the ratio between the number of photoelectrons produced and the number of photons impacting the photoactive surface.

The spectra acquired by means of the monochromator have a field of visibility between 150 and 500 nm, due to limit of the CCD which does not detect wavelength out of this range. The spectra are displayed in a system of Cartesian axes in which the wavelength is shown on the abscissae and the calculated emissivity is shown on the ordinates, expressed in arbitrary units as a function of the intensity of the incident light on a hypothetical specimen whose maximum value is set to 1000.

4. Discussion of results

The experimental tests were carried out at a pressure of 1-3 bara and a temperature of about 1000 °C. During the experiments, images were acquired with the intensified Andor camera and flame emission spectra with the HR460 monochromator.

Before the acquisition of the flame emission spectra, the instrument was calibrated and the optical fiber was aligned with the oxy-combustion chamber. The latter is of crucial importance because the optical fiber transfers the signal to the monochromator, and greater captured optical flux corresponds to greater precision of the spectrum and, consequently, in better measurement of system variables.

In the preliminary phase of the spectra acquisition, it was necessary to carry out the calibration process. Due to the high spatial and temporal variability of the combustion phenomenon, a compromise was sought between an adequate resolution of the spectra and a not-too-high time of integration, which would otherwise only provide us with an average value of the variables under examination.

The following describes the experimental results obtained in 4 tests, whose main parameters are summarized in Table 2.

Table 2: Summary table: different conditions of the experimental tests.

	CH_4 inlet		O_2 inlet		CO_2 inlet		Vapor inlet		Temperature at exhaust	Pressure at exhaust
	[l/min]	[°C]	[l/min]	[°C]	[l/min]	[°C]	[l/min]	[°C]	[°C]	[bara]
Test 1	1.2	20	2.4	20	/	/	/	/	1000	1.0
Test 2	1.2	20	2.4	20	2.5	250	/	/	1000	1.0
Test 3	1.2	20	2.4	20	2.5	250	12.5	250	1000	1.0
Test 4	1.2	20	2.4	20	2.5	250	12.5	250	1000	3.0

The first three tests have been carried out at ambient pressure, while the last one at 3 bara. Besides, the stoichiometric reaction conditions have been assured in all tests.

For each test, the acquisition of flame image was carried out by means of the Andor intensified camera coupled with a 310 nm band pass filter, which allows to view only the OH radicals present inside the combustion chamber.

Each acquisition was repeated 10 times therefore, the image represented below corresponds to an average of the 10 values acquired during the experimental campaign in each condition.

Figure 5 shows the images of flames acquired with the Andor intensified camera. All images present a discontinuity on the left side due to an obstacle in the experimental setup. Particularly, Figure 5a shows a flame which was obtained with CH_4 and O_2 only, under stoichiometric conditions. It has a long and narrow shape and is also characterized by a strong luminous intensity, which means large concentration of OH radicals.

In Test 2 (Figure 5b), CO_2 was added. A comparison between Figure 5a and Figure 5b demonstrates how CO_2 increases the emission of light radiation such that the flame will be less intense and with a slightly more elongated morphology. This result can be explained taking into account that CO_2 partially absorbs radiation.

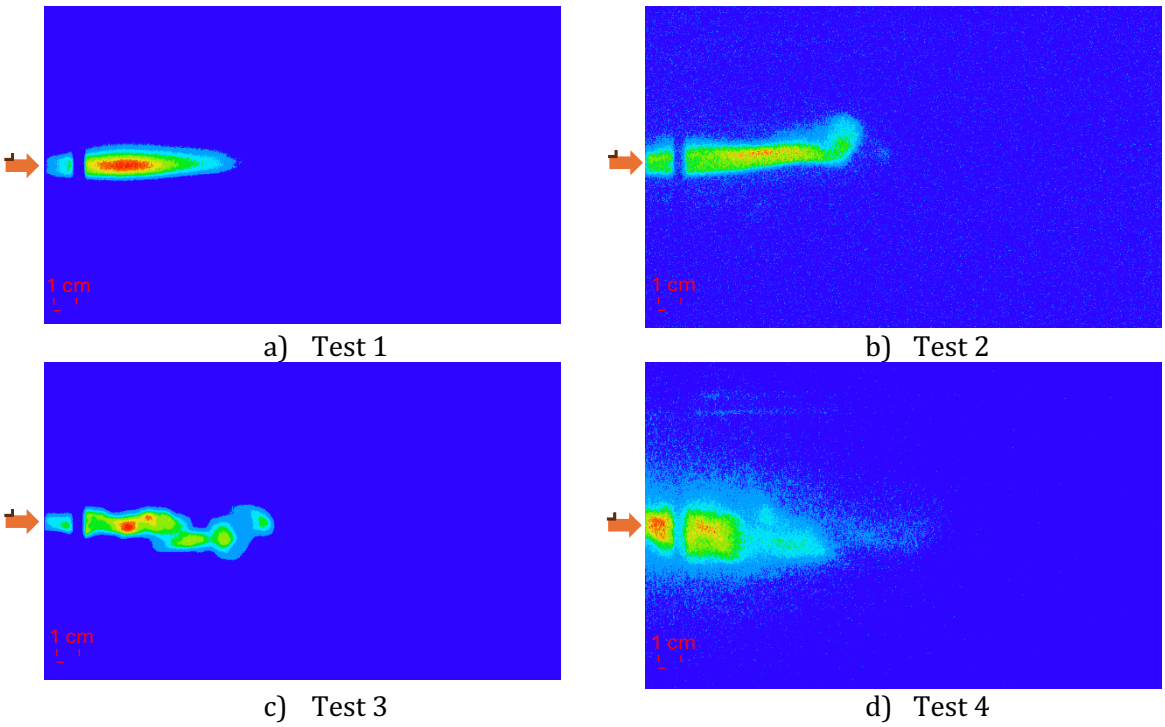

Figure 5: Images of flames acquired with the Andor intensified camera. a) Test 1; b) Test 2; c) Test 3; d) Test 4. The arrows represent the injection point

Figure 5c shows the influence of steam on the oxy-fuel flame. In addition, the flame not only has greater emission of light radiation, but also exhibits instability. In fact, if in Test 1 the flame was regular and mostly symmetrical, with the addition of CO_2 and H_2O gases the flame changes its morphology, becoming more chaotic.

Unlike the previous case, the addition of steam further affects the intensity of the flame and its brightness. In fact, Figure 5c shows a greater concentration of OH radicals.

In the fourth test, the behavior of the flame was studied at a pressure of 3 bara. A comparison between Figure 5c and Figure 5d demonstrated that pressure plays a fundamental role on shape and stability of flame. As the pressure increases, the flame approaches flameless conditions, i.e. the absence of a flame front, therefore combustion could be considered nearly homogeneous, and the flame should occupy almost the entire volume of the chamber. In this case, an enlargement of the flame is clearly visible, although due to the flow of gases along the walls and the excessive length of the combustion chamber, the homogeneity of the flame is not evident throughout the available volume.

In the experimental tests, the emission spectra of flames were also analyzed with the monochromator. Figure 6 shows the emission spectra obtained from the flames in Test 1, Test 2, Test 3 and Test 4 respectively.

Generally speaking, given the analysis of the emission spectra, the intermediate compounds of the combustion reaction can be determined. Figure 6 shows that in all tests, the most evident peaks are around 280 nm, 300 nm 350 nm and 430 nm, which according to Table 1, correspond to CO, OH, CH_3O and CH, respectively. There are also wavelength peaks characteristic of other intermediates such as C_2, C_4H_2, C_6H_6, CHO, CH_2O and CH_3O etc.

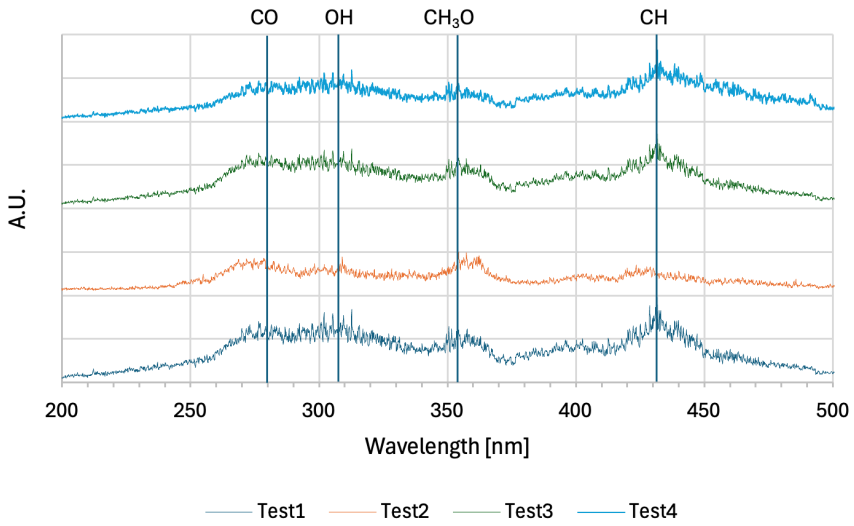

Figure 6: Emission spectra obtained from the difference between the spark light spectrum and the flame emission spectrum. a) TEST 1, b) TEST 2, c) TEST 3 and d) TEST 4.

A comparison between Test 1 and Test 2 states that the contribution of carbon dioxide in the reaction results in a change in the emission spectrum: from a first comparison it can be noted that the oxy-combustion reaction with only oxygen and methane, case a), presents more marked peaks. This behavior may mean that the introduction of CO_2 in the reactor causes a small instability of the flame which translates into a decrease in the formation of OH radicals (whose characteristic wavelengths are 306-309 nm).

The spectrum undergoes a further variation with the addition of steam (graph c). In this case, the formation of all compounds increases, highlighting broader and more defined peaks.

Finally, Test 4 (Figure 6d) shows that the increase in pressure inside the oxy-combustion chamber favors the flameless process. In fact, from its spectrum the peaks are broader than in the previous cases. These results represent a first step in the study of the oxyfuel process, and further measurements need to be carried out to investigate more thoroughly the evolution of the oxyfuel reaction over time.

5. Conclusions

In this work, an experimental setup was developed to study the combustion process in an oxygen atmosphere under conditions of high temperature and high pressure. Due to the transparency of the oxy-combustion chamber, it was possible to determine how the flame front varies, under stoichiometric reaction conditions, first with a 70% recirculation of carbon dioxide, then with the addition of 70 %vol of steam and finally it was studied the behavior of the flame at the pressure of 3 bar.

From this study, it can be said that recirculating gases strongly influence the flame front, but it is the pressure that significantly influences the emission spectrum of the flame and favors the achievement of flameless conditions.

In the different test configurations, the emission spectra of the flames were analyzed, demonstrating a very similar trend with the peaks concentrated between 250 and 500 nm. They

provided information about the intermediate compounds formed during the combustion reaction.

A forthcoming study will focus on analyzing the relationships between the percentage of recirculated CO_2 and vapor and the oxyfuel reaction, how these act on the formation of OH and CH radicals, and how further increase in pressure promotes the complete achievement of the flameless condition. Finally, the effect of any thermoacoustic phenomena on the evolution of the oxyfuel reaction will be studied.

References

[1] Buhre, B.; Elliott, L.; Sheng, C.; Gupta, R.; Wall, T. Oxy-Fuel combustion technology for coal-Fired power generation. Prog. Energy Combust. Sci. 2005, 31, 283–307.
[2] Wall, T.F. Combustion processes for carbon capture. Proc. Combust. Inst. 2007, 31, 31–47.
[3] Perrone, D. A study of oxy-Coal combustion with wet recycle using CFD modeling. In Energy Procedia, Proceedings of the ATI 2015-70th Conference of the ATI Engineering Association, Naples, Italy, 17–20 May 2015; Elsevier: Amsterdam, The Netherlands, 2015; Volume 82, pp. 900–907.
[4] Zheng, L. Oxy-Fuel Combustion for Power Generation and Carbon Dioxide (CO2) Capture; Elsevier: Sawston, Cambridge, 2011.
[5] Colangelo, G., Spirto, G., Milanese, M., de Risi, A. Hydrogen production from renewable energy resources: A case study. Energy Conversion and Management. 2024, 311, 118532.
[6] Milanese, M.; Colangelo, G.; de Risi, A. Progress in CO2 Conversion Using Renewable Energy Sources. Energies 2023, 16, 2350.
[7] E. Koohestanian e F. Shahraki. Review on principles, recent progress, and future challenges for oxy-Fuel combustion CO2. J. Environ. Chem. Eng, vol. 9, p. 105777, 2021.
[8] Simmonds, M.; Miracca, I.; Gerdes, K. Oxyfuel technologies for CO2 capture: A techno-Economic overview. In Greenhouse Gas Control Technologies 7; Elsevier Science Ltd.: Amsterdam, The Netherlands, 2005; pp. 1125–1130.
[9] Raho, B.; Colangelo, G.; Milanese, M.; de Risi, A. A Critical Analysis of the Oxy-Combustion Process: From Mathematical Models to Combustion Product Analysis. Energies2022,15,6514.
[10] Dobó, Z.; Backman, M.; Whitty, K.J. Experimental study and demonstration of pilot-Scale oxy-Coal combustion at elevated temperatures and pressures. Appl. Energy 2019, 252, 113450.
[11] Stanger, R.; Wall, T.; Spörl, R.; Paneru, M.; Grathwohl, S.; Weidmann, M.; Scheffknecht, G.; McDonald, D.; Myöhänen, K.; Ritvanen, J.; et al. Oxyfuel combustion for CO2 capture in power plants. Int. J. Greenh. Gas Control 2015, 40, 55–125.
[12] Yin, C.; Yan, J. Oxy-Fuel combustion of pulverized fuels: Combustion fundamentals and modeling. Appl. Energy 2016, 162, 742– 762.
[13] Choi, S.K.; Kim, J.S.; Chung, S.H. Structure of the edge flame in a methane–Oxygen mixing layer. Combust. Theory Model. 2009, 13, 39–56.
[14] Yin, C.; Rosendahl, L.A.; Kær, S.K. Chemistry and radiation in oxy-Fuel combustion: A computational fluid dynamic modeling study. Fuel 2011, 90, 2519–2529.
[15] Chen, L.; Yong, S.Z.; Ghoniem, A.F. Oxy-Fuel combustion of pulverized coal: Characterization, fundamentals, stabilization and CFD modeling. Prog. Energy Combust. Sci. 2012, 38, 156–214.
[16] Zheng, C.; Liu, Z.; Xiang, J.; Zhang, L.; Zhang, S.; Luo, C.; Zhao, Fundamental and technical challenges for a compatible design scheme of oxyfuel combustion technology. Engineering 2015, 1, 139–149.
[17] Bejarano, P.A.; Levendis, Y.A. Combustion of coal chars in oxygen-Enriched atmospheres. Combust. Sci. Technol. 2007, 179, 1569–1587.
[18] Levendis, Y.A.; Bejerano, P.A. Reaction times of burning bituminous chars at high O2 partial pressures. In Proceedings of the 31st International Technical Conference on Coal Utilization & Fuel Systems, Clearwater, FL, USA, 21–26 May 2006; Sakkestad, B.A.; Eds.; Coal Technology Association: Gaithersburg, MD, USA, 2006, Volume I, pp. 145–157
[19] Smart, J.; O'Nions, P.; Riley, G. Radiation and convective heat transfer, and burnout in oxy-Coal combustion. Fuel 2010, 89, 2468–2476.
[20] Molina, A.; Shaddix, C.R., Hecht E.S., Haynes B.S., Effect of O2/CO2-Firing on Coal Particle Ignition; Sandia National Laboratories (SNL): Albuquerque, NM, USA; Livermore, CA, USA, 2005.